Research Article

The Journal of Anatomical Sciences
Email: journalofanatomicalsciences@gmail.com

J. Anat Sci 17(3) Sept.

Submitted: Jan 31st, 2026
Revised: August 26th, 2026
Accepted: August 31st, 2026

DOI: https://dx.doi.org/10.4314/jans.v17i3.3

Protective Effects of *Momordica charantia* Against Monosodium Glutamate-Induced Ovarian Toxicity in Female Wistar Rats: An *in vivo* and *in Silico* Study

Leviticus O. Arietarhire[1,2], Joseph I. Enya[1,2]*, Samson E. Olorunnado[3], Sherifat O Moshood[4], Angela O. Okosun[5], Sambo A. Jacob[1], Ezekiel O. Hamzat[6], Favour O. Egunjobi[4], Azeezat D. Yakub[4], Ezekiel A. Olugbogi[2], Oladimeji E. Soremekun[2], Toluwanimi O. Afolabi[2,7], Afees J. Olanrewaju[1,2]

[1]Department of Anatomy; [2]Biocomputing and Molecular Department, Eureka Research Lab, Babcock University, Ilishan Remo, Ogun State, Nigeria; [3]Department of Human Anatomy, School of Medicine and Pharmacy, University of Rwanda, Kigali, Rwanda; [4]Department of Anatomy, Faculty of Basic Medical Science, University of Ilorin, Ilorin, Nigeria; [5]Department of Anatomy, Madonna University, Elele, Nigeria; [6]Faculty of Medicine No. 2, Uzhhorod National University, Uzhhorod Ukraine; [7]Department of Anatomy, Olabisi Onabanjo University, Ago-Iwoye, Ogun State, Nigeria.

***Corresponding Author:** Email: enyaj@babcock.edu.ng Tel: 08060931626

ABSTRACT

Monosodium glutamate (MSG) is widely used as a flavor enhancer and has been associated with oxidative and reproductive disturbances in experimental models. This study investigated the protective effects of *Momordica charantia* against MSG-induced ovarian toxicity in adult female Wistar rats using *in vivo and in silico* approaches. Twenty-eight female Wistar rats were randomly assigned into four groups (n = 7): control, *M. charantia* (200 mg/kg), MSG (4 g/kg), and MSG + *M. charantia*. Following treatment, ovarian tissues and blood samples were collected for histological, biochemical, and hormonal analyses. Ovarian superoxide dismutase (SOD), glutathione peroxidase (GPx), and malondialdehyde (MDA), as well as serum follicle-stimulating hormone (FSH), luteinizing hormone (LH), and progesterone, were assessed. Histological changes were evaluated using hematoxylin and eosin staining. In silico screening of M. charantia bioactive compounds against the Keap1–Nrf2 protein–protein interaction was also performed using molecular docking and related drug-likeness/ADMET analyses. MSG administration was associated with reduced SOD and GPx activities, increased MDA levels, altered serum reproductive hormone levels, and marked ovarian histological alterations. Treatment with M. charantia attenuated these changes, with increased SOD and GPx, reduced MDA, improved FSH and LH levels, reduced progesterone, and preservation of ovarian cytoarchitecture. Molecular docking identified rutin, gallic acid, caffeic acid, and hesperidin among the top-performing compounds, with favorable predicted interactions with the Keap1–Nrf2 target. These findings suggest that *M. charantia* attenuates MSG-associated ovarian oxidative, hormonal, and structural alterations, while its constituent compounds show potential interactions with the Keap1–Nrf2 pathway that warrant further experimental investigation.

Keywords: Monosodium glutamate, ovarian toxicity, *Momordica charantia, in silico, in vivo*

INTRODUCTION

Infertility has been on the increase; in addition to other factors, nutrition is a major contributing cause. Poor nutrition can often result in the alteration of normal physiological processes involved in puberty, estrous cycles, and ovarian follicular growth, leading to infertility and susceptibility to various diseases [1]. Many addictive substances used for enhancing, flavoring, and food storage can be potentially harmful due to long-term exposure [2]. Monosodium glutamate (MSG) is an additive used as a flavor enhancer of several types of food, which constitutes a glutamic base and amino acids [3]. Studies reporting growth hormone secretion reduction and high cholesterol levels resulting in stunted growth, obesity, overweight, cardiovascular diseases, neuroendocrine disorder, and subsequently infertility following MSG intake have been well documented [4,5,6,7]. MSG functions normally through the activation of ionotropic and metabotropic glutamate receptors, which could lead to neuronal cell death due to hyperactivation of these receptors as a result of prolonged use of MSG [8,] and can be how it induces neuroendocrine disorders. MSG injection during the first 10 days of neonates using different experimental animals results in a series of neuroendocrine disorders during their adult lives, such as stunted growth, obesity, and decreased fertility [9-12]. Thus, it is of great

importance to investigate novel treatments (especially from plants) for MSG toxicity.

In the recent past, increasing documented evidence has accrued that buttressed the positive roles of herbal medicinal plants in the prevention or control of some metabolic disorders like diabetes, heart diseases, and certain types of cancers [13]. *Momordica charantia* [*M. charantia* (bitter melon)] is a tropical and subtropical cucurbitaceous vine that is widely cultivated in South Asia, India, Africa, China, and the Caribbean. *M. charantia* has been reported to exhibit antidiabetic, antiviral, antitumor, antileukemic, antibacterial, anthelmintic, antimutagenic, antimycobacterial, antioxidant, antiulcer, anti-inflammatory, hypocholesterolemic, hypotriglyceridemic, hypotensive, immunostimulant, and insecticidal properties [14,15]. Hence, it is effective in treating intestinal gas, tumors, wounds, rheumatism, malaria, vaginal discharge, and positive regulation of sugar through the suppression of neural responses to sweet taste stimuli [16]. *M. charantia* has a wide range of applications owing to its unique properties and phytochemical constituents; therefore, it might be effective in treating MSG ovarian toxicity in Wistar rats.

Although previous studies have demonstrated that monosodium glutamate can induce oxidative, hormonal, and structural alterations in reproductive tissues, and that *M. charantia* possesses antioxidant and protective properties, the potential protective effect of *M. charantia* against MSG-induced ovarian toxicity and the molecular mechanisms that may underlie this protection remain insufficiently characterized. In particular, the possible involvement of the Keap1-Nrf2 antioxidant pathway has not been adequately explored in relation to MSG-induced ovarian injury. Therefore, this study investigated the effects of *M. charantia* on MSG-induced alterations in ovarian antioxidant status, lipid peroxidation, reproductive hormone levels and ovarian cytoarchitecture in adult female Wistar rats. In addition, an *in silico* approach was employed to investigate the potential interactions of bioactive compounds from *M. charantia* with the Keap1–Nrf2 protein–protein interaction. We hypothesized that *M. charantia* would attenuate MSG-induced ovarian oxidative, hormonal, and structural alterations, potentially through modulation of antioxidant-related molecular pathways.

MATERIALS AND METHODS

Plant material and extraction

Fresh leaves of *Momordica charantia* were obtained from the Herbarium of the Department of Botany, University of Ilorin, Nigeria. The leaves were washed thoroughly, air-dried at room temperature, and pulverized into a fine powder. The powdered material was extracted by maceration/percolation in distilled water for 5–7 days with intermittent stirring, filtered using muslin cloth, and concentrated at 70°C to obtain the crude aqueous extract [17]. Paste *M. charantia* was prepared in distilled water (40 mg/ml) and adjusted to pH 7.4 with 0.1 M phosphate-buffered saline (PBS) [17]. Crystalline monosodium glutamate MSG (Sigma-Aldrich, USA) was dissolved in distilled water (20 mg/ml) and adjusted to a pH of 7.4 with 0.1 M PBS. Both solutions were freshly prepared each morning of administration and stored at 4ºC before administration.

Animal care, grouping and treatments

Wistar rats (eight weeks old) were kept under standard laboratory conditions, where they had liberal access to rat chow and water. A total of 28 female rats (weight=165±3g) were randomly assigned into 4 groups (A – D, n=7) and treated orally as follows: A – PBS (1 ml daily for 21 days); B – *M. charantia* (200 mg/kg daily for 14 days); C – MSG (4 g/kg daily for 21 days); D – MSG then *M. charantia* (4g/kg MSG daily for 21 days followed by 200 mg/kg *M. charantia* daily for subsequent 14 days). Body weight was measured at baseline and subsequently at 7-day intervals using a calibrated digital weighing balance.

Tissue processing

12 hours after the last administration, rats for histology were euthanized using 20 mg/kg BW of ketamine (intraperitoneal) and subjected to transcardial perfusion in which a flush of 50 ml of 0.1 M PBS (pH 7.4) was followed by 500 ml of 4% paraformaldehyde (PFA). The ovaries were then excised, rinsed in 0.25 M sucrose 3 times for 5 mins each, and then post-fixed in Bouin's solution for 24 hours, after which they were taken for tissue processing. Rats processed for enzymatic and hormonal studies were sacrificed by cervical dislocation (to eliminate the interference of ketamine-induced change in biochemical redox); Blood samples were obtained from the left ventricle of the heart using a 5ml syringe, while the ovaries were then excised, rinsed in 0.25 M sucrose 3 times for 5 min. each and placed in 30% sucrose, in which they were stored at 4°C. After which sections of the ovaries were homogenized in 0.25 M sucrose solution for enzymatic assay.

Biochemical and hormonal assays

Ovarian tissue was homogenized in ice-cold 0.2 M sucrose and centrifuged at 12,000 g/rpm for 10 min at 4°C. The resulting supernatants were collected for biochemical analyses. The activities/concentrations of superoxide dismutase (SOD), glutathione peroxidase (GPx), and malondialdehyde (MDA) were determined using commercially available assay kits obtained from Abcam (USA), according to the manufacturer's

instructions. Serum was separated from whole blood by centrifugation at 12,000 g/rpm for 20 mins and used for determination of follicle-stimulating hormone (FSH), luteinizing hormone (LH), and progesterone using commercially available ELISA kits according to the manufacturer's instructions. Absorbance was measured using a microplate reader, and concentrations/activities were calculated from the appropriate standard curves and expressed in the units specified by the respective assay kits.

Histology and spectrochemistry

Histological staining was carried out in paraffin wax-embedded sections using Hematoxylin and Eosin as described by Fischer *et al.* [18]. Assay kits for superoxide dismutase, glutathione peroxidase, malondialdehyde, Progesterone, follicular stimulating hormone, and luteinizing hormone were procured from Abcam. Lysates from the ovary and blood samples were centrifuged for 10 minutes in a microfuge (IEC: CENTRA-GP8R, DJB Labcare, UK) at 12,000 rpm to obtain supernatants containing organelle fragments and synaptosomes. According to the manufacturer's instructions in the assay kit pack, the supernatants and serum were aspirated into a plainly labeled glass cuvette placed on ice to determine activity.

Data analysis

Results obtained from quantitative studies were analyzed using GraphPad Prism® software (Version 6.1) and tested for analysis of variance (ANOVA) with Tukey's multiple comparisons test. Significance was set at $p<0.05$.

***In-silico* analysis**

To generate and prepare a library of ligands, we began by obtaining 2D structures of bioactive compounds from *M. charantia* [19]. These structures were acquired from various sources, including an online database (https://pubchem.ncbi.nlm.nih.gov) and data obtained through GC-MS and HPLC studies of the plant. For compounds not found in the database, we used ChemDraw to manually draw their structures.

The ligands were then subjected to preparation using the LigPrep function within the Schrödinger suite, utilizing the OPLS3 force field. To establish the ionization states of the compounds, we employed the Epik module, which generated a single stereoisomer for each ligand under conditions of pH 7.0 ± 2.0.

Additionally, we included Keap1-Nrf2 protein-protein interaction (PPI) Co-ligand. This particular co-ligand, identified as (3S)-3-(4-methylphenyl)-3-[2-(5,6,7,8-tetrahydronaphthalen-2-yl)ethanoylamino]propanoic acid) sulfonyl] amino naphthalen-1-Yl] pyrrolidine-3-Carboxylic Acid (SGO) was sourced from PubChem. It underwent the same synthesis procedure as the other ligands and was included in the library for use as a reference ligand.

Protein target retrieval

The 3D crystal structure of the Keap1-Nrf2 protein-protein interaction (PPI) was established using PDB ID: 8IVG20. The target protein underwent several preparations to optimize its suitability for subsequent analyses. Bond instructions were applied, and hydrogen atoms were integrated into the protein structure to ensure completeness and accuracy. The Protein Preparation Wizard in the Schrödinger Suite 2018 was employed to optimize and minimize the protein. Additionally, any missing side chains and loops, not initially present in the structure, were reconstructed to ensure completeness. The protein's tautomeric state was adjusted to match a neutral pH, and further refinement was carried out using the OPLS3 force field, improving the overall quality and stability of the protein structure.

Receptor grid generation

The determination of the active site's size and orientation for protein-ligand docking was carried out through the creation of a receptor grid. Specifically, the scoring coordinates defining the binding pocket of the 8IVG protein were established using Schrödinger Maestro 11.1's receptor grid generation module, as outlined in Olugbogi *et al*., [21]. These coordinates were derived from the co-crystallized ligand and are represented by the x, y, and z grids at 13.93, 63.94, and 28.13, respectively. This step was crucial in defining the region where ligands would be docked and assessed for potential binding interactions.

Molecular docking

We used Schrödinger's Maestro version 11.1 software. The ligands that had been meticulously prepared were subjected to docking simulations with the 8IVG protein, and the resulting data played a pivotal role in subsequent screening steps. HTVS was initially employed to generate a selection of 96 ligands with the highest likelihood of exhibiting a strong binding affinity for 8IVG, selected from a library of 157 compounds sourced from *M. charantia*. Subsequently, these 96 ligands underwent a more rigorous docking process known as XP docking, aimed at pinpointing the bioactive compound and identifying promising hit ligands.

RESULTS

MSG body weight loss was improved by *M. charantia* treatment

Body weight differed among the experimental groups (Fig. 1a). Compared with the control group, MSG

administration resulted in a reduction in body weight, although there was no significance. Treatment with *M. charantia* following MSG exposure significantly attenuated the MSG-associated reduction in body weight. The *M. charantia*-only group differed significantly from the control group ($p<0.05$).

Effects of *M. charantia* on ovarian oxidative stress markers

MSG intake leads to a drop in percentage body weight in comparison to other experimental groups; however, it was only significant when compared to the *M. charantia* group ($p<0.005$), while treatment with *M. charantia* slightly improves the percentage body weight following MSG intake. MDA expression significantly increased due to MSG intake when compared to the CON ($p<0.005$) and *M. charantia* ($p<0.005$) groups, but treatment with *M. charantia* significantly decreased MDA expression in the ovarian homogenate ($p<0.05$). MSG significantly reduced the expression of GPx when compared to the CON ($p<0.005$) and *M. charantia* ($p<0.005$) groups. However, *M. charantia* slightly improves the expression of GPx following MSG intake. MSG causes a marked reduction of SOD expression, which is significant when compared to the CON ($p<0.005$) and *M. charantia* ($p<0.005$) groups, but treatment with *M. charantia* causes a significant increase after MSG intake ($p<0.05$).

Effects of *M. charantia* on serum reproductive hormone levels

There was an upsurge of progesterone in the MSG group, which was significant when compared to the CON ($p<0.005$) and *M. charantia* ($p<0.005$) groups. Treatment with *M. charantia* significantly reduced the level of progesterone after MSG intake ($p<0.01$) (Fig. 2a). The degree of FSH expression was significantly lower due to MSG intake when compared to the CON ($p<0.005$) and *M. charantia* ($p<0.005$) groups; whereas *M. charantia* treatment significantly improved the level of FSH after involvement with MSG ($p<0.05$) (Fig. 2b). Luteinizing hormone level was significantly lower in the MSG group when compared to the CON ($p<0.005$) and *M. charantia* ($p<0.005$) groups. However, interventional measures with *M. charantia* significantly elevated luteinizing hormonal level ($p<0.01$) (Fig 2c).

***M. charantia* normalized the cytoarchitectural changes of the ovary as a result of MSG toxicity**

The characteristic presentations of histological properties of the ovary in this study were demonstrated using the H&E staining technique. At lower magnification, the ovary histological profile of the control groups (CON & *M. charantia*) was devoid of any visible alterations, with consistent layering observable across the groups. Upon closer examination with higher magnification, normal morphology was shown in the control and *M. charantia-treated* groups, as the ovary in these groups shows a wide cortex with numerous primary, secondary, and Graafian follicles, as well as newly formed and degenerated corpora lutea. Histology of ovaries of MSG-treated rats showed cystic degeneration, fibrotically changed stroma, and arteriolar hyalinosis. The ovaries in this group also contain many atretic follicles and no corpora lutea. The ovaries of rats treated with *M. charantia* after MSG-induced toxicity show significant improvement, as their histomorphological characteristics were similar to those of the control and *M. CHARANTIA* groups (Figure 3).

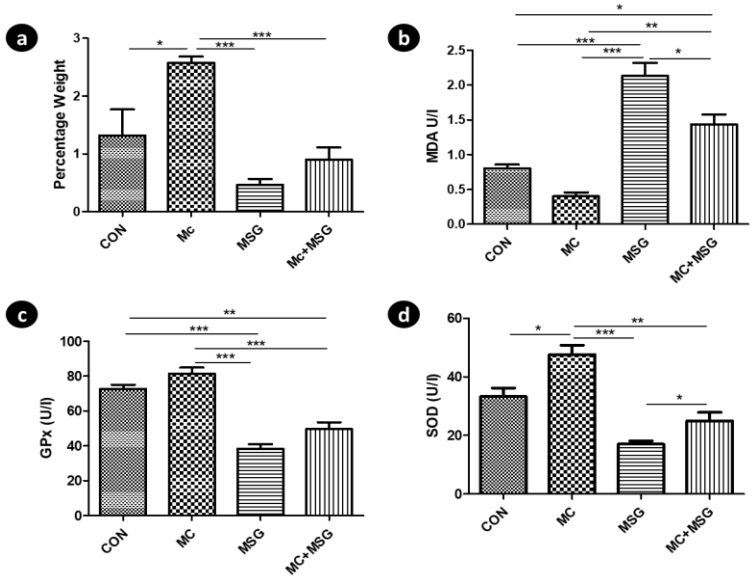

Figure 1a-d: Bar showing the bodyweight and ovarian oxidative redox; Percentage weight (a), MDA (b), GPx (c), and SOD (d), respectively. Bars were plotted with mean ± SD. n=7. Data were analyzed by one-way ANOVA followed by Tukey's test. (* P < 0.05; ** P<0.01; *** P<0.005). Control (CON); *M. charantia* (MC); Monosodium Glutamate (MSG).

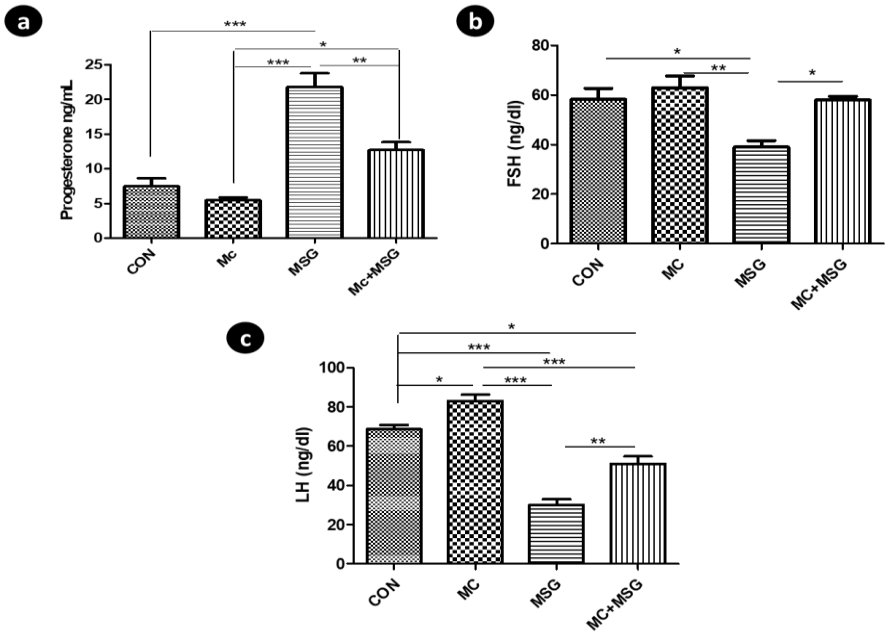

Figure 2a-c: Ovarian viability was shown by measuring reproductive hormones such as progesterone (a), follicle-stimulating hormone (FSH) (b), and luteinizing hormone (LH). Bars were plotted with mean ± SD. n=7. Data were analyzed by one-way ANOVA followed by Tukey's test. (* P < 0.05; ** P<0.01; *** P<0.005). Control (CON); M. charantia (MC); Monosodium Glutamate (MSG).

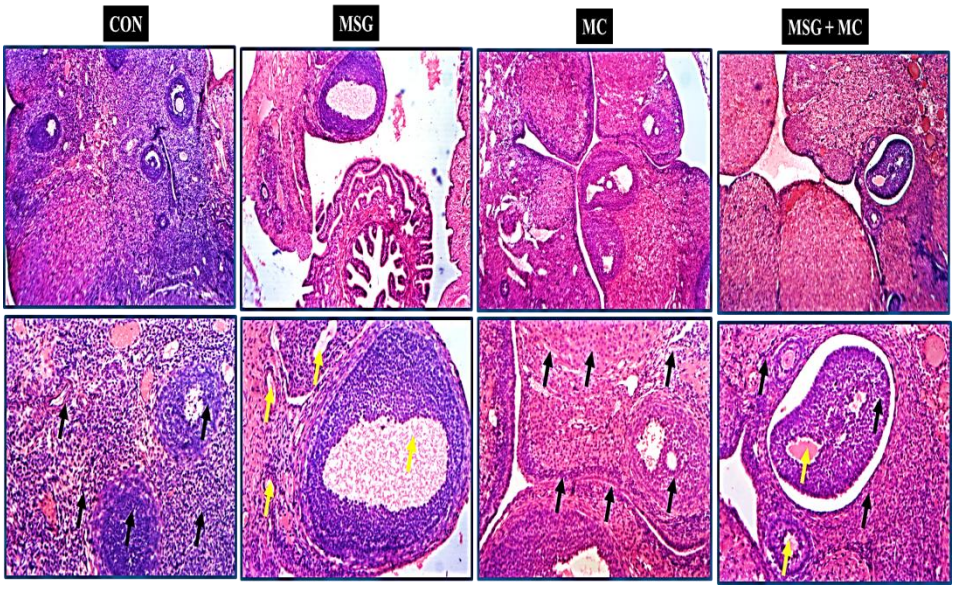

Figure 3: Photomicrography of the ovary showing histomorphological changes across experimental animals at low (x40 MAG) and high (x400 MAG). Normal morphology was shown in the control and the group that was treated with *M. charantia* only, as the ovary in these groups shows a wide cortex with numerous primary, secondary, and Graafian follicles, as well as newly formed and degenerated corpora lutea (black arrow). Histology of ovaries of MSG-treated rats showed cystic degeneration, fibrotically changed stroma, and arteriolar hyalinosis. The ovaries in this group also contain many atretic follicles and no corpora lutea (yellow arrows). The ovaries of rats treated with *M. charantia* after MSG-induced toxicity show significant improvement, as their histomorphological characteristics are similar to those of the control and *M. CHARANTIA* groups.

Distribution of Backbone dihedral Angles of the Prepared Keap1–Nrf2 Protein Structure.

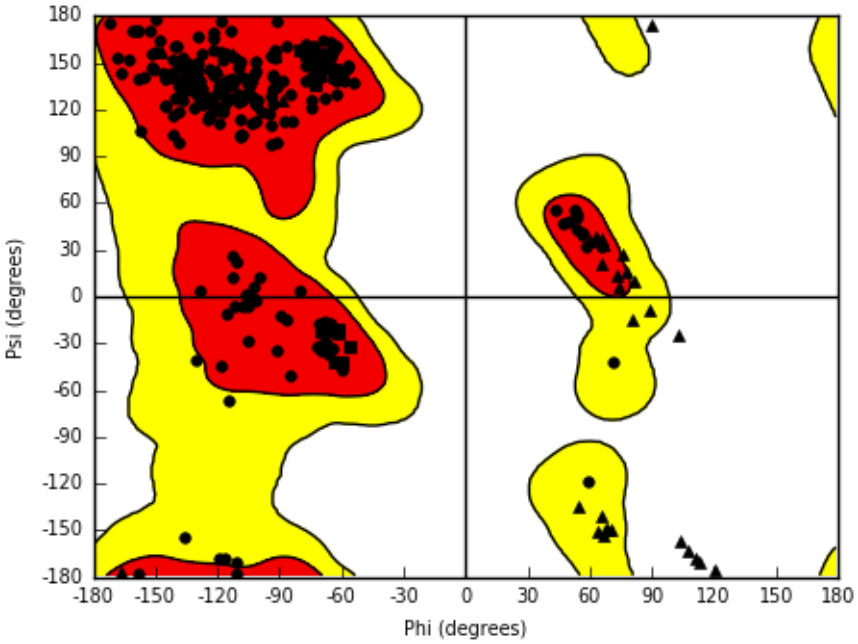

Figure 4: Ramachandran Plot showing the phi and psi degrees. The red region in the Ramachandran Plot represents the forbidden region. The white region is also known as the allowed region. The yellow region is sometimes referred to as the generously allowed region. The black region is located near the center of the plot and represents the energetically most favorable dihedral angle combinations.

Table 1. Docking scores of the top 21 *M. charantia* bioactive compounds against the Keap1–Nrf2 protein–protein interaction

Entry Name	docking score
Rutin	-10.998
SGO	-10.812
Gallic acid	-9.856
Caffeic acid	-9.532
Hesperidin	-9.367
Ferulic acid	-9.253
Syringic acid	-9.219
Arachidic acid	-9.135
Vanillic acid	-9.076
Gadoleic acid	-9.049
Gallocatechin gallate	-8.957
Nonadecanoic acid	-8.698
Beta-resorcylic acid	-8.693
Isoquercitrin	-8.639
Veratric acid	-8.599
Tetracosanoic acids	-8.438
Tetracosanoic acid	-8.438
Lignoseric acid	-8.438
3-coumaric acid	-8.423
p-coumaric acid	-8.423
a-linolenic acid	-8.372

Table 2: A heatmap displaying the docking scores (XP GScore), van der Waals energy (glide evdw), total energy (glide energy), hydrogen bonding (XP HBond), binding free energy (MMGBSA dG Bind), and molecular weight (mol MW) of ligands derived from *M. charantia*.

Entry Name	XP GScore	glide evdw	glide energy	XP HBond	MMGBSA dG Bind	mol MW
Rutin	-11.027	-41.436	-62.454	-4.601	-49.3	610.524
SGO	-10.812	-39.56	-56.204	-4.051	-80.58	351.444
Gallic acid	-9.863	-10.899	-26.084	-4.689	-28.88	170.121
Caffeic acid	-9.532	-18.224	-32.889	-3.81	-39.59	180.16
Hesperidin	-9.367	-34.561	-51.944	-5.225	-35.79	610.568

Table 3: A heatmap illustrating the SASA (Solvent Accessible Surface Area), PISA (Protein Interfaces, Surfaces, and Assemblies), hydrogen bond donors (donorHB), hydrogen bond acceptors (accptHB), QPlogHERG (Predicted Logarithm of the HERG Potassium Channel Inhibition), and QPPCaco (Predicted Caco-2 Permeability) values for ligands docked from *M. charantia*.

Entry Name	SASA	PISA	donorHB	accptHB	QPlogHERG	QPPCaco
Rutin	848.666	189.026	9	20.55	-6.025	0.323
SGO	649.541	163.6	1	3.5	-1.83	93.856
Gallic acid	346.597	91.799	4	4.25	-1.541	9.622
Caffeic acid	388.937	146.972	3	3.5	-2.157	22.094
Hesperidin	915.519	174.68	7	20.05	-6.368	2.135

Table 4: A heatmap displaying the QPlogBB, QPPMDCK, QPlogKhsa, human oral absorption, percent human oral absorption, and rule of five values for ligands originating from *M. charantia*.

Entry Name	QPlogBB	QPPMDCK	QPlogKhsa	Human Oral Absorption	Percent Human Oral Absorption	Rule of Five
Rutin	-5.551	0.083	-1.397	1	0	3
SGO	-1.054	77.649	0.43	3	88.182	0
Gallic acid	-1.708	4.158	-0.984	2	41.244	0
Caffeic acid	-1.55	10.213	-0.803	2	54.172	0
Hesperidin	-4.831	0.642	-1.183	1	0	3

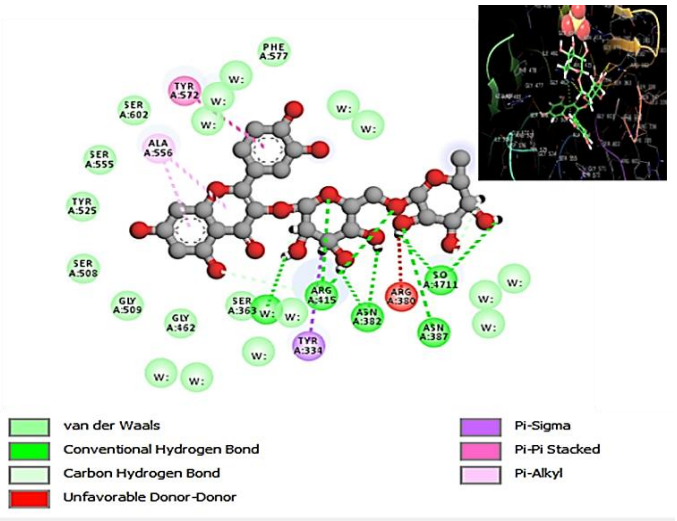

Figure 5a: Visual depiction of the 2D and 3D structural arrangements of Rutin within the binding site of the Keap1/Nrf2

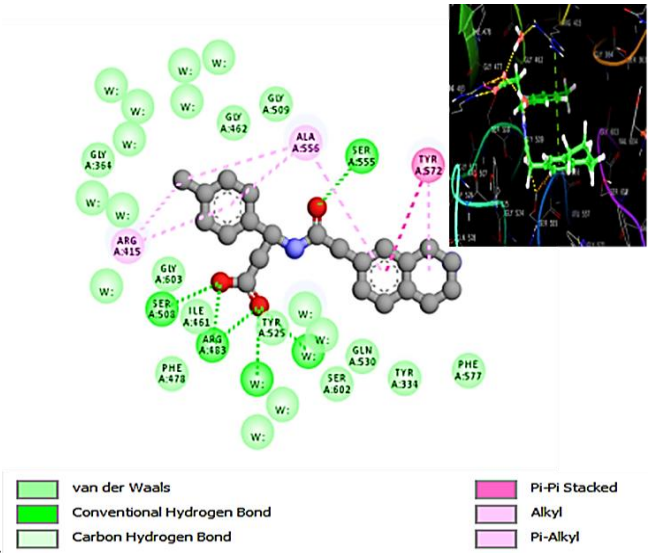

Protein-Protein Interaction (PPI).

Figure 5b: Visual representation illustrating the 2D and 3D structural configurations of SGO (co-ligand) within the active site of the Keap1/Nrf2 Protein-Protein Interaction (PPI).

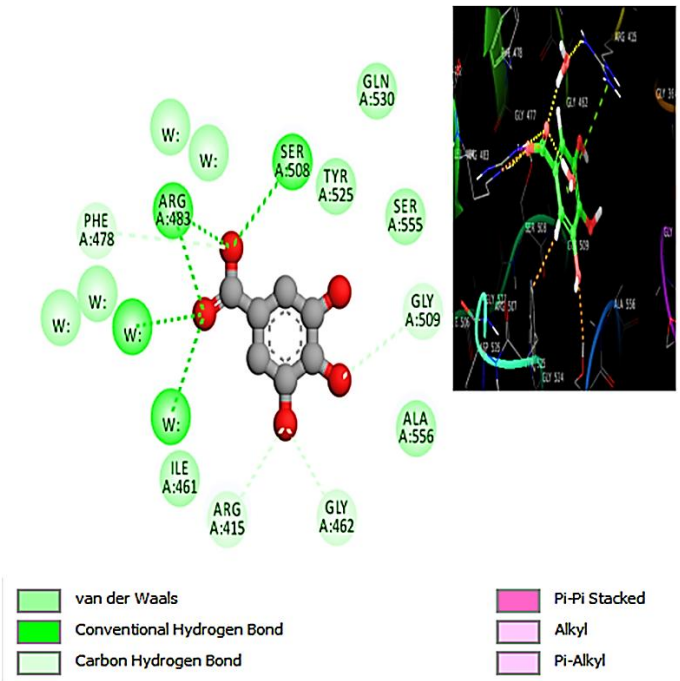

Figure 5c: Visual depiction showcasing the 2D and 3D structural arrangements of gallic acid when docked into the active site of the Keap1/Nrf2 Protein-Protein Interaction (PPI).

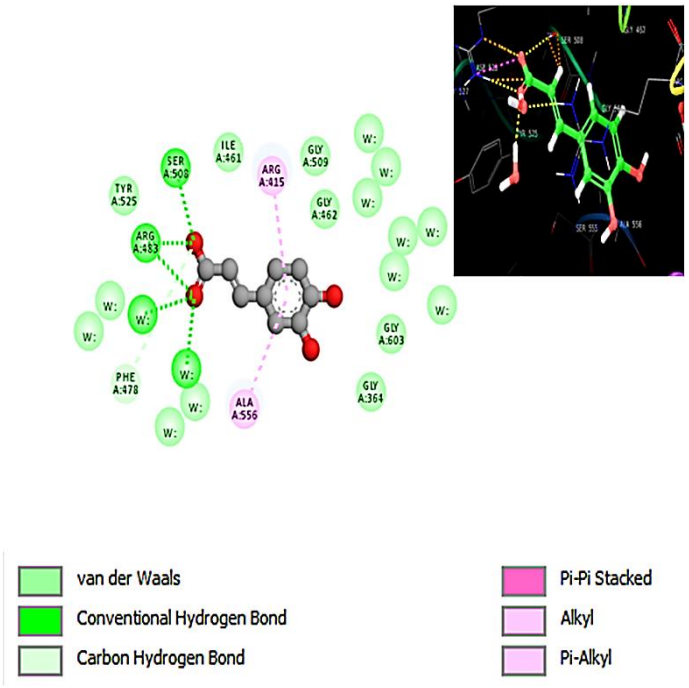

Figure 5d: Illustrative presentation illustrating the 2D and 3D structural configurations of caffeic acid within the active site of the Keap1/Nrf2 Protein-Protein Interaction (PPI).

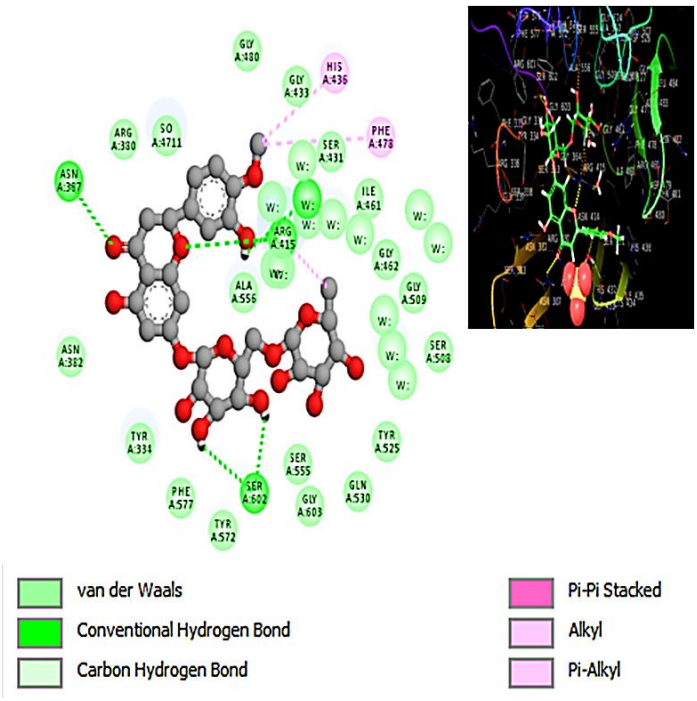

Figure 5e: Visual depiction showcasing the 2D and 3D molecular structures of hesperidin situated within the active site of the Keap1/Nrf2 Protein-Protein Interaction (PPI).

DISCUSSION

Monosodium glutamate (MSG) exposure has been associated with oxidative and reproductive disturbances in experimental models. In the present study, MSG administration produced ovarian alterations characterized by reduced antioxidant activity, increased lipid peroxidation, disruption of reproductive hormone levels, and marked histological changes. Treatment with *Momordica charantia* attenuated these alterations, suggesting a protective effect against MSG-induced ovarian toxicity.

The reduction in ovarian SOD and GPx activities accompanied by increased MDA levels following MSG administration indicates an imbalance between oxidative processes and endogenous antioxidant defense. These findings are consistent with previous reports linking MSG exposure to oxidative stress and lipid peroxidation in experimental animals [22–24]. The improvement in SOD and GPx activities and reduction in MDA following *M. charantia* treatment suggest that the extract may enhance ovarian antioxidant defense and limit oxidative damage. This effect may be related to the phytochemical constituents of *M. charantia*, including flavonoids and phenolic compounds, which have been reported to possess antioxidant properties [25,26–29]. However, the present study did not directly determine which individual constituents were responsible for the observed effects.

MSG administration also altered serum reproductive hormone levels, with increased progesterone and reduced FSH and LH levels. These changes may indicate disruption of the hypothalamic-pituitary-ovarian axis. Previous studies have reported that MSG can interfere with reproductive function through mechanisms involving oxidative stress and excitotoxicity [30]. In the present study, *M. charantia* treatment partially restored FSH and LH levels and reduced the MSG-associated increase in progesterone. The hormonal improvement may be related, at least in part, to attenuation of oxidative stress; however, the present study did not directly investigate hypothalamic or pituitary mechanisms, and therefore this interpretation should be considered cautiously.

Histological examination further demonstrated the protective effect of *M. charantia*. Ovaries from MSG-treated animals showed cystic degeneration, stromal fibrosis, arteriolar hyalinosis and increased atretic follicles, whereas ovaries from animals receiving *M. charantia* following MSG exposure showed comparatively preserved cytoarchitecture. Similar protective effects of *M. charantia* against tissue injury have been reported in other experimental models and have been associated with its antioxidant and anti-inflammatory properties [25,31]. The present findings extend these observations by demonstrating preservation of ovarian morphology following MSG exposure.

The *in silico* findings provide preliminary insight into a possible molecular basis for the antioxidant effects observed in vivo. The Keap1–Nrf2 pathway is an important regulator of cellular antioxidant responses, with Keap1 regulating Nrf2 stability under basal conditions [20,32,33]. Molecular docking identified rutin, gallic acid, caffeic acid, and hesperidin among the compounds with favorable predicted interactions with the Keap1–Nrf2 protein–protein interaction, with rutin producing the most favorable docking score among the selected compounds. Several hydrogen-bond, van der Waals, and other non-covalent interactions were identified between the compounds and residues within the target interface.

The docking and ADMET analyses also revealed differences in the predicted drug-like properties of the investigated compounds. Rutin and hesperidin exceeded some of the evaluated hydrogen-bonding and Lipinski parameters, while differences were observed in predicted permeability and oral absorption. These findings suggest that favorable docking scores alone should not be interpreted as evidence of therapeutic efficacy, since pharmacokinetic properties and biological activity must also be established experimentally.

The molecular interaction analysis further showed that several compounds shared interactions with residues including ARG415, ASN387, ARG483 and SER508. Rutin and hesperidin demonstrated hydrogen-bond interactions involving ARG415 and ASN387, while gallic acid and caffeic acid showed interactions involving ARG483 and SER508. These observations suggest that selected *M. charantia* constituents may interact with the Keap1–Nrf2 interface. Nevertheless, the docking analysis provides only a computational prediction and does not establish that these compounds inhibit Keap1–Nrf2 binding or activate Nrf2 in vivo. Experimental studies involving protein-binding assays and measurement of Nrf2-related signaling are therefore required to validate this proposed mechanism.

Overall, the present findings indicate that *M. charantia* attenuated MSG-associated ovarian oxidative, hormonal and structural alterations. The convergence of the in vivo findings with the predicted interactions of selected *M. charantia* compounds with the Keap1–Nrf2 interface provides a basis for further investigation, but the molecular mechanism should not be considered established until experimentally validated.

CONCLUSION

In conclusion, *Momordica charantia* attenuated MSG-induced ovarian toxicity by improving antioxidant status, reducing lipid peroxidation,

normalizing reproductive hormone alterations and preserving ovarian cytoarchitecture in female Wistar rats. In silico findings further identified selected *M. charantia* bioactive compounds, particularly rutin, gallic acid, caffeic acid and hesperidin, as potential interactors of the Keap1–Nrf2 protein–protein interaction, although these predicted molecular interactions require experimental validation.

Conflict of interest

The authors have no conflicts of interest to declare

REFERENCES

1. Bernard SA, Gray TW, Buist MD, Jones BM, Silvester W, Gutteridge G, *et al*. Treatment of comatose survivors of out-of-hospital cardiac arrest with induced hypothermia. N Engl J Med. 2002;346(8):557-63.
2. Inetianbor JE, Yakubu JM, Ezeonu SC. Effects of food additives and preservatives on man: a review. Asian J Sci Technol. 2015;6(2):1118-35.
3. Win DT. MSG-flavor enhancer or deadly killer. AU JT. 2008;12(1):43-49.
4. Ikonomidou C, Turski L. Excitotoxicity and neurodegenerative diseases. Curr Opin Neurol. 1995;8(6):487-97.
5. Eskes R, Antonsson B, Osen-Sand A, Montessuit S, Richter C, Sadoul R, et al. Bax-induced cytochrome C release from mitochondria is independent of the permeability transition pore but highly dependent on Mg2+ ions. J Cell Biol. 1998;143(1):217-24.
6. Rodríguez-Reinoso F. The role of carbon materials in heterogeneous catalysis. Carbon. 1998;36(3):159-75.
7. Parsons RB, Waring RH, Ramsden DB, Williams AC. In vitro effect of the cysteine metabolites homocysteic acid, homocysteine and cysteic acid upon human neuronal cell lines. Neurotoxicology.1998;19:599-603.
8. Ibiyeye R, Sulaimon F, Imam A, Adana M, Okesina A, Ajao M. Phoenix dactylifera and polyphenols ameliorated monosodium glutamate toxicity in the dentate gyrus of Wistar rats. Niger J Physiol Sci. 2023;38(1):73-78.
9. Olney JW, Ho OL. Brain damage in infant mice following oral intake of glutamate, aspartate or cysteine. Nature. 1970;227(5258):609-11.
10. Burde RM, Schainker B, Kayes J. Acute effect of oral and subcutaneous administration of monosodium glutamate on the arcuate nucleus of the hypothalamus in mice and rats. Nature. 1971;233(5314):58-60.
11. Olney JW. Monosodium glutamate effects. Science. 1971;172(3980):294.
12. Reynolds WA, Bingel AS, Lemkey-Johnston N. Female sterility in the MSG-induced hypothalamic lesion of the mouse [abstract]. Presented at: 19th Annual Meeting of the Society for Gynecological Investigation; 1972. p. 46.
13. Wang ZQ, Zhang XH, Yu Y, Poulev A, Ribnicky D, Floyd ZE, *et al*. Bioactives from bitter melon enhance insulin signaling and modulate acyl carnitine content in skeletal muscle in high-fat diet-fed mice. J Nutr Biochem. 2011;22(11):1064-73.
14. Fang EF, Ng TB. Bitter gourd (Momordica charantia) is a cornucopia of health: a review of its credited antidiabetic, anti-HIV, and antitumor properties. Curr Mol Med. 2011;11(5):417-36.
15. Thenmozhi AJ, Subramanian P. Antioxidant potential of Momordica charantia in ammonium chloride-induced hyperammonemic rats. Evid Based Complement Alternat Med. 2011;2011:612023.
16. Taylor MF, Suckling KF, Rachlinski JJ. The effectiveness of the Endangered Species Act: a quantitative analysis. BioScience. 2005;55(4):360-67.
17. Jain A, De S. Aqueous extraction of bitter gourd (Momordica charantia L.) juice and optimization of operating conditions. Fruits. 2016;71(6):379-87.
18. Fischer G, Kostic S, Nakai H, Park F, Sapunar D, Yu H, et al. Direct injection into the dorsal root ganglion: technical, behavioral, and histological observations. J Neurosci Methods. 2011;199(1):43-55.
19. Afroz S, Fairuz S, Joty JA, Uddin MN, Rahman MA. Virtual screening of functional foods and dissecting their roles in modulating gene functions to support post COVID-19 complications. J Food Biochem. 2021;45(12):e13961.
20. Otake K, Ubukata M, Nagahashi N, Ogawa N, Hantani Y, Hantani R, et al. Methyl and Fluorine Effects in Novel Orally Bioavailable Keap1–Nrf2 PPI Inhibitor. ACS Med Chem Lett. 2023;14(5):658-665. doi:10.1021/acsmedchemlett.3c00067.
21. Olugbogi EA, Bodun DS, Omoseeye SD, Onoriode AO, Oluwamoroti FO, Adedara JF, *et al*. Quassia amara bioactive compounds as a novel DPP-IV inhibitor: an in silico study. Bull Natl Res Cent. 2022;46(1):1-14.
22. Carter BE, Monsivais P, Perrigue MM, Drewnowski A. Supplementing chicken broth with monosodium glutamate reduces hunger and desire to snack but does not affect

energy intake in women. Br J Nutr. 2011;106(9):1441-8.
23. Shi Z, Wittert GA, Yuan B, Dai Y, Gill TK, Hu G, *et al*. Association between monosodium glutamate intake and sleep-disordered breathing among Chinese adults with normal body weight. Nutrition. 2013;29(3):508-13.
24. Ibegbulem CO, Chikezie PC, Ukoha AI, Opara CN. Effects of diet containing monosodium glutamate on organ weights, acute blood steroidal sex hormone levels, lipid profile and erythrocyte antioxidant enzyme activities of rats. J Acute Dis. 2016;5(5):402-7.
25. Jia S, Shen M, Zhang F, Xie J. Recent advances in Momordica charantia: functional components and biological activities. Int J Mol Sci. 2017;18(12):2555.
26. Padmashree A, Sharma GK, Semwal AD, Bawa AS. Studies on the antioxygenic activity of bitter gourd (Momordica charantia) and its fractions using various in vitro models. J Sci Food Agric. 2011;91(4):776-82.
27. Tripathi UN, Chandra D. The plant extracts of Momordica charantia and Trigonella foenum graecum have antioxidant and anti-hyperglycemic properties for cardiac tissue during diabetes mellitus. Oxid Med Cell Longev. 2009;2(5):290-6.
28. Tripathi UN, Chandra D. Anti-hyperglycemic and anti-oxidative effect of aqueous extract of Momordica charantia pulp and Trigonella foenum graecum seed in alloxan-induced diabetic rats. Indian J Biochem Biophys. 2010;47(4):227-33.
29. Deng Y, Tang Q, Zhang Y, Zhang R, Wei Z, Tang X, et al. Protective effect of Momordica charantia water extract against liver injury in restraint-stressed mice and the underlying mechanism. Food Nutr Res. 2017;61(1):1348864.
30. Ochiogu I, Ogwu D, Uchendu C, Okoye C, Ihedioha J, Mbegbu E. Effects of monosodium-L-glutamate administration on serum levels of reproductive hormones and cholesterol, epididymal sperm reserves and testicular histomorphology of male albino rats. Acta Vet Hung. 2015;63(1):125-39.
31. Abas R, Othman F, Thent ZC. Protective effect of Momordica charantia fruit extract on hyperglycaemia-induced cardiac fibrosis. Oxid Med Cell Longev. 2014;2014:429060.
32. Kaspar JW, Niture SK, Jaiswal AK. Nrf2: INrf2 (Keap1) signaling in oxidative stress. Free Radic Biol Med. 2009;47(9):1304-9.
33. Banerjee A, Mukherjee S, Maji BK. Worldwide flavor enhancer monosodium glutamate combined with high lipid diet provokes metabolic alterations and systemic anomalies: an overview. Toxicol Rep. 2021;8:938-961.